DRAFT VERSION JULY 5, 2016
Preprint typeset using LaTeX style emulateapj v. 01/23/15

arXiv:1607.00440v1 [astro-ph.IM] 2 Jul 2016

THE SERENDIP III 70 CM SEARCH FOR EXTRATERRESTRIAL INTELLIGENCE

STUART BOWYER, MICHAEL LAMPTON, ERIC KORPELA, JEFF COBB, MATT LEBOFSKY, AND DAN WERTHIMER
Space Sciences Laboratory, University of California, Berkeley, CA 94720
Draft version July 5, 2016

ABSTRACT

We employed the SERENDIP III system with the Arecibo radio telescope to search for possible artificial extraterrestrial signals. Over the four years of this search we covered 93% of the sky observable at Arecibo at least once and 44% of the sky five times or more with a sensitivity of $\sim 3 \times 10^{-25} Wm^{-2}$. The data were sent to a 4×10^6 channel spectrum analyzer. Information was obtained from over 10^{14} independent data points and the results were then analyzed via a suite of pattern detection algorithms to identify narrow band spectral power peaks that were not readily identifiable as the product of human activity. We separately selected data coincident with interesting nearby G dwarf stars that were encountered by chance in our sky survey for suggestions of excess power peaks. The peak power distributions in both these data sets were consistent with random noise. We report upper limits on possible signals from the stars investigated and provide examples of the most interesting candidates identified in the sky survey. *This paper was intended for publication in 2000 and is presented here without change from the version submitted to ApJS in 2000.*

Keywords:

1. INTRODUCTION

Early radio searches for extraterrestrial intelligence used dedicated telescope time to search for emission from nearby stars (see Tarter 1991 for a partial listing, and Tarter 2001 for a full listing of these searches). This type of search became increasingly difficult to carry out at major facilities because of a general reluctance to devote dedicated telescope time to such projects, which though interesting, are acknowledged to have a low probability of success. In addition, sky surveys were carried out which scanned substantial portions of the sky. The Berkeley SERENDIP project (Search for Extraterrestrial Radio Emissions from Nearby Developed Intelligent Populations) solved the dedicated telescope time problem by using data obtained simultaneously with ongoing astronomical research. This program began over twenty years ago (Bowyer et al. 1983) and has continued to the present day with ever increasing sensitivity and an ever-widening set of search parameters.

Other sky surveys using dedicated telescopes have been, and are continuing to be, carried out. The Ohio State program (Dixon 1985) was the earliest sky survey; this project is now terminated. The Harvard search (Leigh & Horowitz 1997) has also been terminated. The Argentinian search (Lemarchand et al. 1997), and the Australian search (Stootman et al. 1999) continue. Targeted searches of nearby stars have been initiated by the SETI Institute (Tarter 1997) using substantial amounts of dedicated telescope time which were obtained in return for a substantial financial contribution to the telescope upgrade which was carried out after the conclusion of the SERENDIP III observations.

We discuss our sky survey search for artificial extraterrestrial signals with the SERENDIP III system (Bowyer et al. 1997) and the Arecibo telescope. Although the search was a sky survey, nearby solar-type stars inevitably fell within the beam pattern of the telescope in the course of these observations. As part of the analysis of the SERENDIP III data, we have separately investigated the data from observations of the sky coincident with these nearby stars. Although our integration times for individual targets are relatively short (as compared, for example, with the SETI Institute targeted search), our sensitivity is still substantial because of the large collecting area of the Arecibo telescope and the outstanding receivers that are available for use with this instrument.

We report the results of our sky survey and provide upper limits on possible signals from stars in this paper.

2. OBSERVATIONS AND ANALYSIS

The SERENDIP III data were obtained with the National Astronomy Ionosphere Center's radio observatory in Arecibo, Puerto Rico with a 430 MHz receiver. Data collection began in April, 1992 and ended in October, 1998.

The feed used for SERENDIP III was located at the opposite carriage house from the primary observer's feed. This resulted in three observation modes. In the first, representing about 45% of the observing time, the primary observer's feed was tracking a point on the sky. This resulted in the SERENDIP III beam moving across the sky at roughly twice the sidereal rate. In the second, representing about 40% of the observing time the feeds were stationary, resulting in motion at the sidereal rate. In the third, representing about 15% of the observing time, the SERENDIP III feed was tracking a point on the sky.

Power spectra were generated by the SERENDIP III four million channel spectrum analyzer which had a 1.7 second integration period and a 0.6 Hz frequency resolution (2.5 MHz instantaneous band coverage). The sensitivity achieved in a 1.7 second integration at our typical system temperature of 45 K was 3×10^{-25} W m^{-2}. This bin size is wide enough to encompass Doppler frequency drifts caused by the Earth's motions plus reasonable accelerations of a hypothetical transmitter's reference frame. The receiver's entire 12 MHz band was processed in 2.4 MHz steps taking about 8.5 seconds to complete a single sweep. The SERENDIP III fast Fourier transform based hardware is described in detail by Werthimer, et al. (1997).

Adaptive thresholding was achieved by baseline smoothing the raw power spectra with a sliding eight thousand channel local-mean boxcar and searching for channels exceeding 16 times the mean spectral power. These signals were recorded

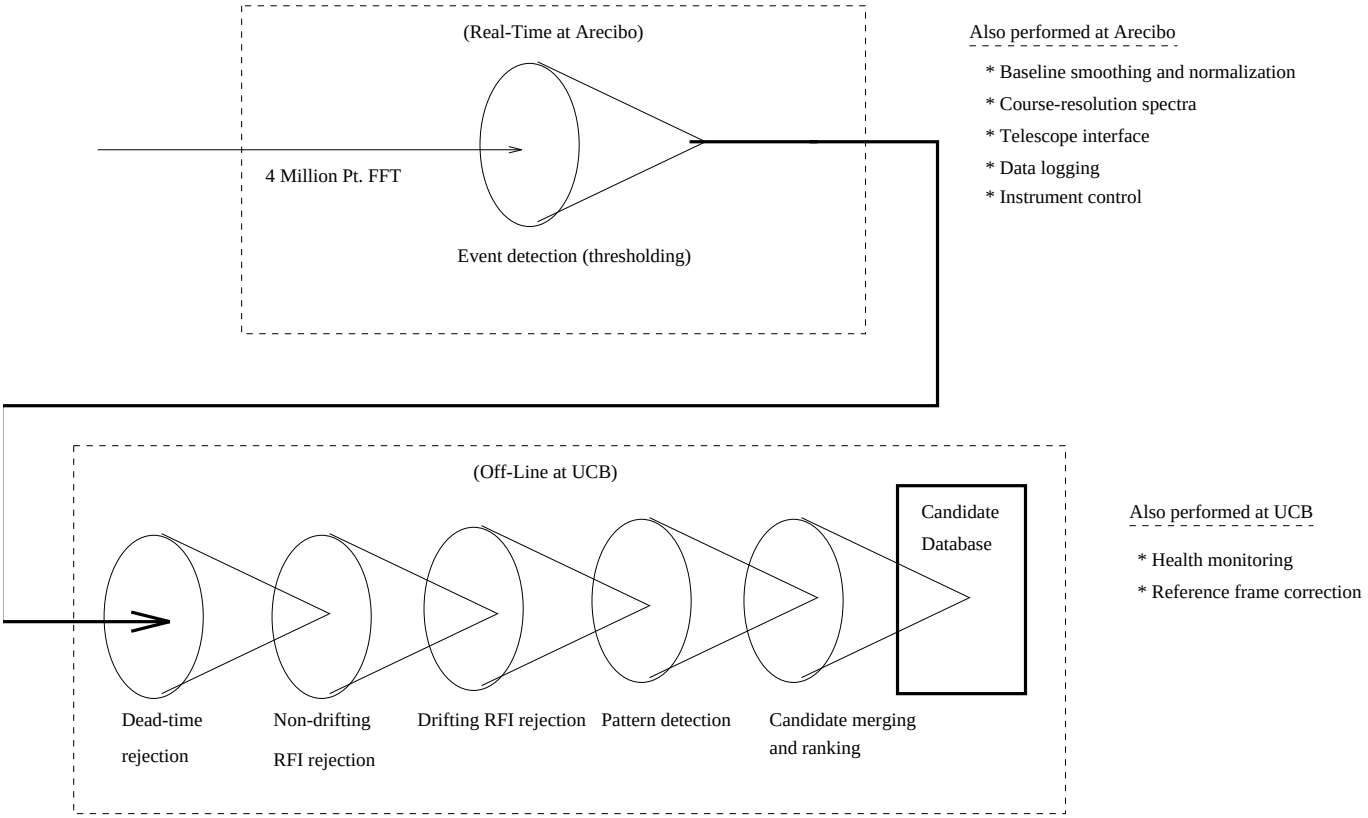

Figure 1. An illustration for the SERENDIP III data flow showing the steps taken to detect candidate signals. Real-time processing consists of power spectra generation and application of an adaptive threshold to the resulting spectra. Off-line data reduction included RFI rejection techniques, pattern detection, and candidate extraction.

along with time, pointing coordinates, detection frequency, and signal power.

Following the real-time data analysis by the SERENDIP III instrument, the reduced data was shipped to Berkeley of off-line data reduction and candidate generation. Off-line data reduction included radio frequency interference (RFI) rejection techniques, pattern detection, and candidate extraction. The overall data flow is shown in Figure 1.

2.1. *Off-line Data Reduction*

Data were transferred from Arecibo to Berkeley across the Internet where off-line data analysis activities began. Data reduction consisted of removing data taken during periods when the telescope was slewing too fast or too slow for our analysis procedures, followed by the application of a suite of RFI filters.

Excessively rapid telescope slew rates precluded acquisition of accurate positioning information. In addition, during times when the receiver tracks a point on the sky, it is not possible for our analysis programs to differentiate between continuous RFI and a potential signal. Therefore, our first filter was to censor data acquired during periods of rapid telescope movement and periods when the telescope was tracking sky objects. Roughly 15% of the data were removed for this reason.

The next step in data reduction was non-drifting RFI rejection. SERENDIP's non-drifting RFI rejection algorithms incorporated dynamically adaptive statistical analysis routines that detect spurious signals from terrestrial and near-space sources. Three cluster analysis tests were conducted on each input data file spanning several hours of observation. Signals were rejected if they (1) were detected over broad areas of the spectrum in one or more integration periods (broad spectrum interference), (2) persisted at the same receiver frequency through multiple telescope beams, or (3) persisted in the same channel of the spectrum analyzer.

Broad spectrum interference was identified by the rejection test:

$$x > 50 \quad and \quad \frac{\sum d^2}{x} > S \tag{1}$$

where d is the number of frequency bins (0.6 Hz/bin) between simultaneous events above the threshold and x is the number of events above threshold in the spectrum. For SERENDIP III, the threshold value was set at $S = 10^8$.

RFI rejection algorithm (2) uses a statistical method to determine if several detections at the same observing frequency could be ruled out. If these detections occur with a significantly above-average hit rate, and they continue to occur when our observing beam has moved beyond one beam width (0.17 degrees), we reject the hypothesis of random Poisson events being the cause. Instead we mark these detections as being due to external RFI, and reject them.

RFI rejection algorithm (3) uses the same statistical test as (2) but applies it to hit sequences that have the same intermediate-frequency bin number. In this way it rejects interference generated within the observatory.

Data surviving the first three rejection criteria were further analyzed for RFI that drifts rapidly in frequency and were therefore not rejected by algorithms (2) and (3) above. Figure 2 illustrates SERENDIP's drifting frequency RFI detection al-

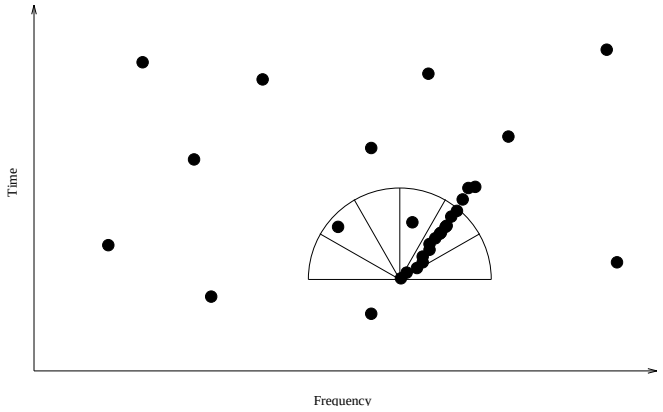

Figure 2. Schematic illustration of SERENDIP's drifting RFI detection algorithm. Sectors of frequency-time space around each detection were analyzed for signals that exhibit time-coherency and persistence over multiple pointings of the telescope's beam.

gorithm. The average event density in frequency-time space was calculated for each data set. Sectors in frequency-time space around each detection (shown as dots in Figure 2) were analyzed to identify sectors having an unusually high number of detections. Sectors containing an excessive number of detections were further analyzed for the presence of drifting signals that persisted through multiple pointings of the telescope beam.

An example of the efficacy of the RFI rejection techniques is shown in Figure 3. Note that after application of SERENDIP's RFI filters, the remaining data closely approached the number expected from a Poisson noise distribution. Typically, 98% of the RFI was rejected, yet only 1% of the band was lost during RFI removal.

2.2. *Pattern Detection*

A suite of pattern detection algorithms was employed to detect signal recurrence and telescope beam pattern matching. The primary pattern looked for was recurrence of a signal in frequency over time and position. All data were frequency corrected to the solar system barycenter. Thus, only those signals that displayed the proper Doppler drift relative to the solar system barycenter remained at a nearly constant frequency. If a signal recurred within a defined frequency window, it was tagged as a candidate. We defined frequency windows of two different widths in order to find two different classes of signals.

The first class (Class I) consists of signals with no frequency drift in the barycentric frame. If transmitted from a planet, such a signal must contain a Doppler correction, and therefore would be a deliberately beamed message. For such signals, the chief cause of potential frequency drift arises from our lack of knowledge of the source's exact position on the sky. We use the direction of the beam center to approximate the source position, and obtain an approximate compensating frequency drift by projecting our antenna's diurnal and annual acceleration onto that nominal line of sight. Due to our beam's size (0.17 degrees), this drift rate uncertainty can shift an ideal signal by as much as 120 Hz. Consequently, our compensated signal class defined a candidate as any set of signals that recurred within a band whose width $f_\sigma = 120$ Hz.

The second class (Class II) consists of signals containing significant Doppler acceleration. Radio leakage from a transmitter on a planet will significantly drift in frequency over

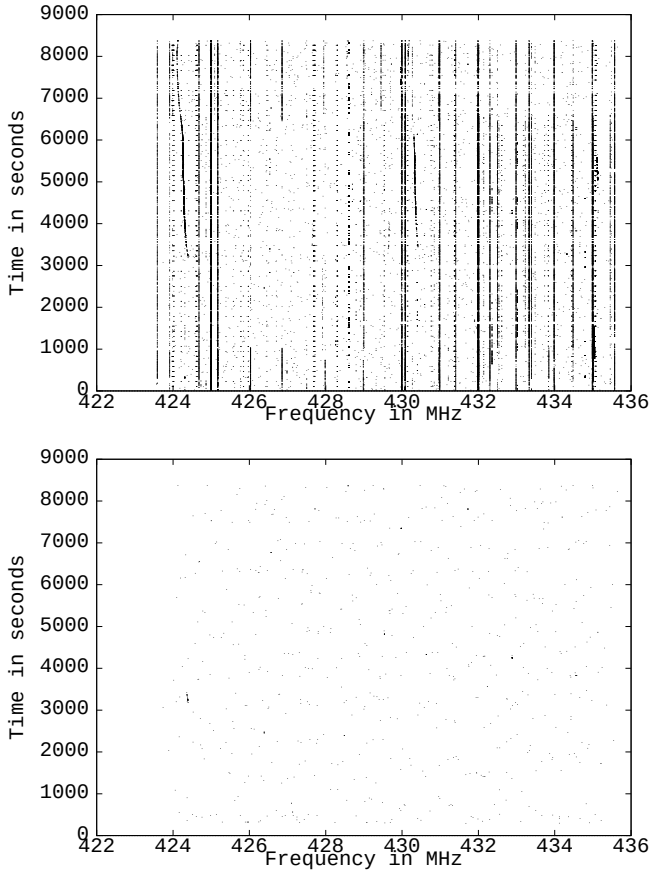

Figure 3. Data from a period of severe interference (top). Each dot represents a high power signal detection by the SERENDIP instrument. After RFI filtering (bottom) the number of hit remaining approaches that expected from a Poisson distribution, as would be expected in a white-noise environment.

time spans of minutes to months. Here, signal sets were allowed a frequency deviation $f_\sigma = 50$ kHz. The width of this band was derived assuming a transmitter whose acceleration was as great as the Jovian cloud tops.

Multiple detections in a given transit were examined to determine if the observed power as a function of time matched the telescope's Gaussian beam pattern. Such a finding would suggest that the signal emanated from a point source on the sky.

2.3. *Candidate Merging and Ranking*

The output of SERENDIP's suite of pattern detection algorithms was a collection of statistically interesting events. These data sets were then examined to identify candidate locations for signals of interest. A candidate was defined as a one beamwidth area on the sky that was identified by one or more pattern detection algorithms. A candidate is fully described by one or more records in the candidate database, each of which is the result of detection by a single algorithm. In addition, celestial objects such as nearby stars, globular clusters, and known planetary systems are entered into the candidate database to check for coincidence with candidates identified by the other algorithms described herein.

Candidates are ranked by two methods. First, each candidate record was given an algorithm specific score. Second, we asked how many algorithms detected the candidate. Here we considered coincidence with an interesting celestial object to be counted as an "algorithm".

To determine the score in the case of multiple transit detections, we calculated the relative probability of our detections occurring from noise, given the number of detections in the candidate area, the number of times we have observed the candidate area, the number of frequency bins searched by the algorithm, and the actual frequency separation of the detections. The relative probability is given by

$$P = \frac{n_e^{n_d}}{n_d!\left(\frac{F_{tot}}{F_{win}}\right)^{(n_d-1)}}\left[\frac{\Delta f + f_\sigma}{f_\sigma}\right] \quad (2)$$

where:
n_e is the total number of events logged at any frequency in the candidate area,
n_d is the number of detections within F_{win},
F_{win} is the frequency window searched for events,
F_{tot} is the total SERENDIP band observed,
Δf is the maximum frequency separation for the detection set,
f_σ is the expected frequency variance as explained in section 2.3.
In searches for either Class I or Class II signals, the lower the numerical rating in this algorithm, the more promising the candidate.

To calculate the score in the case of beam pattern matching in a single transit across the telescope's Gaussian beam, we first determined the best fit Gaussian to the data. The relative score is then given by

$$P_G = A_G\ Q(\chi^2 \mid \nu) \quad (3)$$

where A_G is the amplitude of the best fit Gaussian, and $Q(\chi^2 \mid \nu)$ is the χ^2 probability function. In this case, the higher the numerical rating, the more promising the candidate.

The data from the most promising candidates were independently scrutinized for RFI contamination by three researchers and those surviving this evaluation constitute the list of most interesting candidates. Our top candidates from our signal detection algorithms and their scores are given in Table 1.

2.4. *Investigation of Possible Signals from Nearby G-Dwarf Stars*

We investigated the data obtained from nearby G-dwarf stars that were observed by chance in our sky survey with the rationale that these were especially interesting candidates. In this effort, we used the Center for Astrophysics list of G-dwarf stars within (roughly) 100pc of the Sun (Latham 1999) as listed on their web site as of August 1999[1]. We identified those stars in this list visible with the Arecibo telescope (i.e. stars between -2° and$+38^\circ$). We then searched the SERENDIP III position data set and identified stars in the list that fell within the half power beam width of the Arecibo antenna during our observations.

Of the 516 stars in the CFA list that are observable with the Arecibo telescope, 494 had been observed at least once, and 439 had been observed multiple times. In Figure 4 we show a histogram of the number of times these stars were observed.

We derived upper limits to the excess power from these stars by first checking the most recent version of the Hipparcos catalogue for the stellar distances. The number of stars observed versus distance is shown in Figure 5. We then derived the upper limits to the source stellar luminosity using

[1] http://cfa-www.harvard.edu/∼latham/gdwarf.html

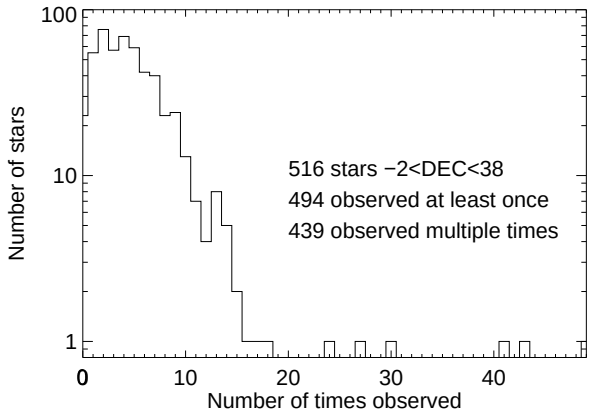

Figure 4. A histogram of the number of separate times each star in the CFA G-dwarf subset was observed in the SERENDIP III search. No narrow band excess power beyond that expected for random noise was detected from these stars.

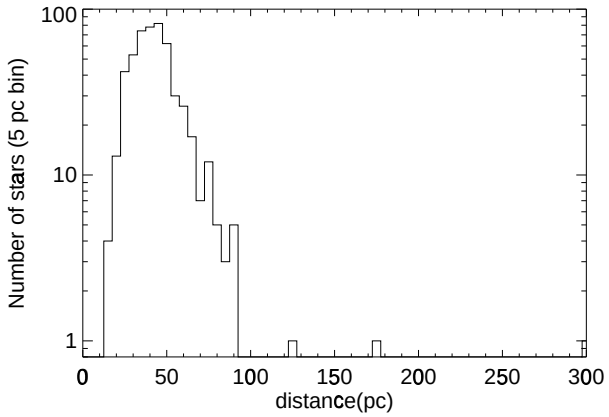

Figure 5. A histogram showing the Hipparcos distance distribution of stars in the CFA G-dwarf subset.

the Hipparcos distances and the observed fluxes. We note that the sensitivity limits are uncertain to a factor of two because we used the average sensitivity of the antenna rather than the sensitivity at the exact position of the star within the beam.

In Table 2 we provide the HD number of the observed stars, their distances as obtained from the Hipparcos catalogue, and the upper limits to the irradiated power at the star.

3. CONCLUSIONS

We have carried out an extensive search with the world's largest telescope for evidence of radio emission produced by an extraterrestrial intelligence. We were able to carry out this search using this unique facility because of the non-intrusive character of our observing program. A major challenge in our search (and in all other searches for extra terrestrial intelligence) is the problem of false signals produced as a result of human activity. We developed a variety of techniques to deal with this problem and demonstrated their robustness. This shows that a non-intrusive collateral data collection technique such as ours is viable.

Given the extensive character of our search we found many signals of potential interest. A prioritization scheme was developed to identify the most promising of these signals. These

Table 1
Most Interesting Candidates

R.A. (hours)	Dec (deg)	Sky Separation (deg)	Frequency (MHz)	Max. Freq. Separation[1] (Hz)	# of Obs.[2]	# of Times Detected	Score by Algorithm[3] 1	2	3	Coincident Object
0.67	28.1	0.1	429.600	6	6	2	91.084			GJ 1019
0.96	7.8	0.1	426.839	-	1	1			43.17	
2.13	26.9	0.1	431.959	17	20	3	1.801			
4.59	27.0	0.1	434.603	30	13	3	0.632			
5.13	2.1	0.2	435.009	46467	4	2		79.371	22.68	
8.15	9.0	0.1	435.089	-	1	1			26.93	GJ 299
10.23	18.5	0.2	430.059	79	34	3	20.525			
14.32	25.9	0.2	427.350	72	8	3	0.250			
23.09	26.8	0.1	429.973	27	21	3	2.529			

[1] Maximum frequency separation between multiple observations
[2] Number of times SERENDIP III observed this point in the sky
[3] Three different scoring algorithms:
Algorithm 1: Doppler compensated signal class (120Hz max frequency window) (see eq. 2); smaller is more remarkable
Algorithm 2: Non-Doppler compensated signal class (50kHz max frequency window) (see eq. 2); smaller is more remarkable
Algorithm 3: Gaussian beam fit (see eq. 3); larger is more remarkable

were examined in more detail. In the end, no extraterrestrial signals were identified. We do not find this surprising nor discouraging given our lack of knowledge as to appropriate source locations, frequencies and time periods that an intentional extraterrestrial signal may be employing.

We are continuing our search.

We thank the Arecibo staff for their support in carrying out this project which they did as an after-hours volunteer project. The Arecibo Observatory is part of the National Astronomy and Ionosphere Center which is operated by Cornell University under a Cooperative Agreement with the National Science Foundation. We acknowledge the efforts of the many volunteers who have worked on SERENDIP over the years. We acknowledge a generous gift by Watson and Marilyn Alberts to carry out this analysis of the SERENDIP data. This analysis has also been supported by grants from the SETI Institute and the Planetary Society. The SERENDIP III project was supported by significant contributions from Mrs. Elizabeth Bowyer, the Planetary Society, and the Toshiba Corporation. Additional support was provided by Intel, Xilinx, and the Friends of SERENDIP.

REFERENCES

Bowyer, S., Zeitlin, G., Tarter, J., Lampton, M., & Welch, W 1983, Icarus, 53, 147

Bowyer, S., Werthimer, D., Donnelly, C., Cobb, J., Ng, D., & Lampton, M. 1997, in Astronomical and Biochemical Origins and the Search for Life in the Universe, ed. C. Cosmovici, S. Bowyer and D. Werthimer (Bologna: Editrice Compositori), 667

Cobb, J., Donnelly, C., Bowyer, S., Werthimer, D., & Lampton, M., 1997, in Astronomical and Biochemical Origins and the Search for Life in the Universe, ed. C. Cosmovici, S. Bowyer and D. Werthimer (Bologna: Editrice Compositori), 677

Dixon, R. 1985, in The Search for Extraterrestrial Life: Recent Developments, ed. M. Papagiannis (Dordrecht: D. Reidel Publishing Co.), 305

Leigh, D. & Horowitz, P. 1997, in Astronomical and Biochemical Origins and the Search for Life in the Universe, ed. C. Cosmovici, S. Bowyer and D. Werthimer (Bologna: Editrice Compositori), 601

Latham, D. 1999, in Bioastronomy 99: A New Era in Bioastronomy, ed. G Lemarchand and K. Meech (Astronomical Society of the Pacific), 19

Lemarchand, G., Colomb, F. R., Hurrell, E. E., & Olalde, J. C. 1997, in Astronomical and Biochemical Origins and the Search for Life in the Universe, ed. C. Cosmovici, S. Bowyer and D. Werthimer (Bologna: Editrice Compositori), 611

Stootman, F. H., de Horta, A. Y., Wellington, K. J. & Oliver, C. 1999, in Bioastronomy 99: A New Era in Bioastronomy, ed. G Lemarchand and K. Meech (Astronomical Society of the Pacific), 90

Tarter, J. C. 1991, in Frontiers of Life, Third Recontres de Blois, ed. J. and K. Tran Tranh Van, J. C. Mounolou, J. Schneider, C. McKay (France: Editions Frontieres), 351

Tarter, J. C. 1997, in Astronomical and Biochemical Origins and the Search for Life in the Universe, ed. C. Cosmovici, S. Bowyer and D. Werthimer (Bologna: Editrice Compositori), 633

Tarter, J. C. 2001, ARA&A, in preparation

Werthimer, D., Bowyer, S., Ng, D., Donnelly, C., Cobb, J., Lampton, M., & Airieau, S. 1997, in Astronomical and Biochemical Origins and the Search for Life in the Universe, ed: C. Cosmovici, S. Bowyer and D. Werthimer (Bologna: Editrice Compositori), 683

Table 2
Stars observed with SERENDIP III

HD number	Distance (pc)	Upper Limit EIRP ($\log_{10}$(Watts))
101	38	12.7
377	40	12.8
531E	70	13.2
531W	70	13.2
700	54	13.0
1832	41	12.8
4903	53	13.0
5035	39	12.7
6715	33	12.6
7047A	40	12.7
8009A	65	13.2
8009B	65	13.2
8262	26	12.4
8523	60	13.1
8574	44	12.8
8648	45	12.9
9091	46	12.9
9224	43	12.8
9472	33	12.6
9670	37	12.7
9986	26	12.4
10126	34	12.6
10844	54	13.0
11045	58	13.1
11130	27	12.4
11850	33	12.6
12235	31	12.5
12783	48	12.9
13357A	49	12.9
13357B	49	12.9
13382	33	12.6
13483	34	12.6
13836	37	12.7
13997	34	12.6
14082B	39	12.7
14305	34	12.6
14348	62	13.1
14651	40	12.8
14874	59	13.1
15632	42	12.8
16086	54	13.0
16397	36	12.7
17674	47	12.9
17820	65	13.2
18144	26	12.4
18330	39	12.7
18702	32	12.6
18774	66	13.2
19019	23	12.3
19308A	43	12.8
19445	39	12.7
19518	41	12.8
19902	42	12.8
19962	38	12.7
20165	22	12.2
20477	52	13.0
21183	75	13.3
21663A	46	12.9
21774	50	13.0
22309	45	12.9
23314	49	12.9
24040	47	12.9
24053	33	12.6
24206	179	14.1
24496	21	12.2
24552	45	12.9
24702	47	12.9
25295	65	13.2
25682	46	12.9
25825	47	12.9
26749	36	12.7
26756	46	12.9
26767	45	12.9
26913	21	12.2
26923	21	12.2

Table 2 — *Continued*

HD number	Distance (pc)	Upper Limit EIRP ($\log_{10}$(Watts))
27282	47	12.9
27406	45	12.9
27642	62	13.1
27732	48	12.9
27771	47	12.9
27859	48	12.9
28099	47	12.9
28205	46	12.9
28237	47	12.9
28258	47	12.9
28344	47	12.9
28406B	46	12.9
28462	40	12.8
28474	53	13.0
28580	36	12.7
28676	39	12.7
28992	43	12.8
29150	34	12.6
29356	63	13.1
29461	48	12.9
30101E	43	12.8
30101W	43	12.8
30246	51	13.0
30286	32	12.6
30508	48	12.9
30589	51	13.0
30974	51	13.0
31000	28	12.5
31253	54	13.0
31412	36	12.7
31501	33	12.6
31867	28	12.4
32070	39	12.7
32237	29	12.5
32259	38	12.7
32347	54	13.0
33021A	28	12.5
33334NE	47	12.9
33334SW	47	12.9
33636	29	12.5
33866	47	12.9
34445	45	12.9
34590	58	13.1
34745	37	12.7
35147	50	13.0
35769	57	13.1
36308	36	12.7
36443	38	12.7
36667	57	13.1
37271	48	12.9
37685	73	13.3
37773	38	12.7
38230A	21	12.2
39570A	54	13.0
39881A	28	12.4
40040	68	13.2
40616	54	13.0
41708	45	12.9
42160	45	12.9
42618	23	12.3
43587A	19	12.1
43947	28	12.4
44985	33	12.6
45391	26	12.4
45580	48	12.9
45759	50	13.0
46375	33	12.6
47127	27	12.4
48684	54	13.0
50060	87	13.4
51219	32	12.6
51295	42	12.8
52456	28	12.5
53505	58	13.1
53532	44	12.8
54046	46	12.9

Table 2 — *Continued*

HD number	Distance (pc)	Upper Limit EIRP ($\log_{10}$(Watts))
54100	45	12.9
54351	44	12.8
54405	46	12.9
54718	46	12.9
55458A	25	12.4
55918	38	12.7
56202	53	13.0
56303	41	12.8
56513	35	12.7
58781	30	12.5
58971	43	12.8
59360	41	12.8
59374	50	13.0
60298	39	12.7
62346	51	13.0
63935	50	12.9
64090	28	12.5
64324	35	12.6
65629	32	12.6
66348A	43	12.8
66485	44	12.8
66550	38	12.7
68168	34	12.6
68284	300	14.5
69056	38	12.7
70088	43	12.8
70571A	92	13.5
70571B	92	13.5
72946	23	12.3
73226	43	12.8
73668A	36	12.7
74011	46	12.9
74156	65	13.2
74567	93	13.5
75302	30	12.5
76218	26	12.4
76261	46	12.9
76349	49	12.9
76752	40	12.8
76765	61	13.1
76780	34	12.6
77024A	77	13.3
77278	31	12.5
77407	30	12.5
78317	48	12.9
78660	50	13.0
79498A	49	12.9
79726	48	12.9
80408	39	12.7
80536	51	13.0
80870	45	12.9
81040	33	12.6
82140	59	13.1
82939	38	12.7
83408	58	13.1
84209	72	13.3
84749	47	12.9
85426	61	13.1
85689	45	12.9
86133A	42	12.8
86133B	42	12.8
86460	41	12.8
86794	52	13.0
87680	39	12.7
88371	62	13.1
88446	69	13.2
88725	36	12.7
89055	36	12.7
89307	31	12.5
89813	27	12.4
90164	54	13.0
90905	32	12.6
91148	37	12.7
91204	52	13.0
93215	47	12.9
94028	52	13.0

Table 2 — *Continued*

HD number	Distance (pc)	Upper Limit EIRP ($\log_{10}$(Watts))
94292	77	13.3
94426	53	13.0
95177	49	12.9
95364	82	13.4
95366	59	13.1
95980	53	13.0
96094	60	13.1
96497	53	13.0
96574	50	13.0
96679	66	13.2
96937	31	12.5
98078	41	12.8
98697	43	12.8
99404	53	13.0
99419	45	12.9
99505	33	12.6
100180A	23	12.3
100180B	23	12.3
101242	34	12.6
101444	41	12.8
103111	78	13.3
103847	29	12.5
104243	36	12.7
104923	40	12.7
104956	51	13.0
105087	58	13.1
105844	43	12.8
106156	31	12.5
106210	34	12.6
106252	37	12.7
106366	66	13.2
106510	51	13.0
107146	29	12.5
107705A	30	12.5
107705B	30	12.5
108653	51	13.0
108874	69	13.2
109628A	84	13.4
109628B	84	13.4
111398A	36	12.7
111470	56	13.1
112001	55	13.0
112257	42	12.8
112735	58	13.1
112756	53	13.0
112959A	59	13.1
113319	31	12.5
114060A	37	12.7
114060B	37	12.7
114174	26	12.4
114606	61	13.1
115231	53	13.0
115273	49	12.9
115349	45	12.9
115382	91	13.5
115519	61	13.1
115755	34	12.6
115762A	60	13.1
116442	16	12.0
116443	17	12.0
116497	49	12.9
117858	60	13.1
118659	53	13.0
119054	50	12.9
119056	61	13.1
119550	60	13.1
120553	44	12.8
121298NW	75	13.3
121298SE	75	13.3
121320	33	12.6
122518	55	13.0
122652	37	12.7
123033B	44	12.8
124019	49	12.9
124677A	36	12.7
125056	42	12.8

Table 2 — *Continued*

HD number	Distance (pc)	Upper Limit EIRP ($\log_{10}$(Watts))
126246A	36	12.7
126246B	36	12.7
126512	47	12.9
126583	34	12.6
126961	41	12.8
127825	58	13.1
128219	68	13.2
129209	50	13.0
129413A	40	12.8
129814	42	12.8
130268	68	13.2
131179	39	12.7
132973	75	13.3
133161	35	12.7
134066A	32	12.6
134066B	32	12.6
135101A	28	12.5
135101B	28	12.5
135792A	43	12.8
136925	46	12.9
138246	62	13.1
138573	31	12.5
138919	41	12.8
139018	79	13.3
139324	53	13.0
139457	47	12.9
139839	65	13.2
140209	65	13.2
140233	78	13.3
140324	55	13.0
140514	83	13.4
140750	68	13.2
141272	21	12.2
141529	55	13.0
142093	31	12.5
142229	41	12.8
142637	66	13.2
143291	26	12.4
144873	47	12.9
145229	33	12.6
145729	45	12.9
146588	45	12.9
146644	61	13.1
147044	36	12.7
147528	51	13.0
147750	40	12.8
148530	47	12.9
148816	41	12.8
149028	48	12.9
149380	94	13.5
149890	39	12.7
150554A	45	12.9
150828B	63	13.2
150933A	44	12.8
152264	64	13.2
153627	43	12.8
153701	37	12.7
154417	20	12.2
154656	42	12.8
154931	55	13.0
155060	36	12.7
155193	61	13.1
155358	43	12.8
155423	44	12.8
156146	76	13.3
156893	68	13.2
156968	55	13.0
157089	39	12.7
157637	41	12.8
158226A	69	13.2
158331	51	13.0
158332	30	12.5
159909	37	12.7
160013	42	12.8
161728	63	13.2
161848	38	12.7

Table 2 — *Continued*

HD number	Distance (pc)	Upper Limit EIRP ($\log_{10}$(Watts))
162209	53	13.0
163609A	50	12.9
164595	29	12.5
165173	33	12.6
165476	45	12.9
165672	44	12.8
166301	35	12.6
167081A	49	12.9
169359	60	13.1
169748A	52	13.0
169822	27	12.4
169889	38	12.7
170294	58	13.1
170469	65	13.2
171009	70	13.2
171067	25	12.4
171620	52	13.0
172310	36	12.7
172649	47	12.9
172867	66	13.2
173548A	52	13.0
173548B	52	13.0
174457	55	13.0
174719	28	12.5
175726	27	12.4
177305	43	12.8
178911B	49	12.9
180684	59	13.1
181047A	50	13.0
182619	33	12.6
182758	66	13.2
183341	45	12.9
183970	50	13.0
184403	44	12.8
184592	42	12.8
186704A	30	12.5
187123	48	12.9
187548	45	12.9
187882	76	13.3
187897	33	12.6
187923A	28	12.4
188015	53	13.0
188510	39	12.7
189067	43	12.8
189087	25	12.4
190404	16	11.9
190516A	44	12.8
190594	43	12.8
190605	44	12.8
190609	44	12.8
191672	69	13.2
192367	129	13.8
195019A	37	12.7
195034	28	12.5
196201	38	12.7
196885A	33	12.6
198089	39	12.7
198416	60	13.1
200466E	44	12.8
200466W	44	12.8
200565	64	13.2
200746	44	12.8
201219	36	12.7
201891	35	12.7
202072	49	12.9
202108	27	12.4
203030	41	12.8
204277	34	12.6
204712	61	13.1
205702	57	13.1
206332	50	13.0
206374	27	12.4
206387A	55	13.0
206658	48	12.9
207740	49	12.9
209262A	46	12.9

Table 2 — *Continued*

HD number	Distance (pc)	Upper Limit EIRP ($\log_{10}$(Watts))
209458	47	12.9
209858	55	13.0
209875	51	13.0
210388	43	12.8
210460	56	13.0
210462A	54	13.0
210483	49	12.9
210553	45	12.9
211476	31	12.5
211786	42	12.8
212291	32	12.6
212858	55	13.0
214059	80	13.4
214435	49	12.9
214560	55	13.0
215257	42	12.8
215274	45	12.9
216625	44	12.8
216631	43	12.8
217165	44	12.8
218133	38	12.7
218172	74	13.3
218261	28	12.5
219172	46	12.9
220008	87	13.4
220077	77	13.3
220255	52	13.0
220334B	37	12.7
220773	48	12.9
221477	59	13.1
221822	39	12.7
221851	23	12.3
221876	75	13.3
222033	50	13.0
222941A	46	12.9
223061	45	12.9
223238	47	12.9
224156	29	12.5
225261	26	12.4